From Ants to Fishing Vessels: A Simple Model for Herding and Exploitation of Finite Resources

José Moran,[1,2,3,4,*] Antoine Fosset,[1,3] Alan Kirman,[2] and Michael Benzaquen[1,3,5]

[1]*Chair of Econophysics and Complex Systems, Ecole polytechnique, 91128 Palaiseau Cedex, France*
[2]*Centre d'Analyse et de Mathématique Sociales, EHESS, 54 Boulevard Raspail, 75006 Paris, France*
[3]*LadHyX UMR CNRS 7646, Ecole polytechnique, 91128 Palaiseau Cedex, France*
[4]*Complexity Science Hub Vienna, Josefstädter Straße 39, A-1080, Austria*
[5]*Capital Fund Management, 23 Rue de l'Université, 75007 Paris, France*

(Dated: September 22, 2020)

We analyse the dynamics of fishing vessels with different home ports in an area where these vessels, in choosing where to fish, are influenced by their own experience in the past and by their current observation of the locations of other vessels in the fleet. Empirical data from the boats near Ancona and Pescara shows stylized statistical properties that are reminiscent of Kirman and Föllmer's ant recruitment model, although with two ant colonies represented by the two ports. From the point of view of a fisherman, the two fishing areas are not equally attractive, and he tends to prefer the one closer to where he is based. This piece of evidence led us to extend the original ants model to a situation with two asymmetric zones and finite resources. We show that, in the mean-field regime, our model exhibits the same properties as the empirical data. We obtain a phase diagram that separates high and low herding regimes, but also fish population extinction. Our analysis may have interesting policy implications for the ecology of fishing areas.

I. INTRODUCTION

A problem of general interest is that of the individual and collective exploitation of a resource. Depending on the particular context, the dynamics can be very different. A crucial factor is the effect of the behaviour of individuals on the collective outcome. In financial markets for example, the decision to buy may enhance the value of the resource for others as the price of an asset may increase as the demand for it grows. This positive feedback can lead to "herd behaviour" and to creation of "bubbles". If, on the other hand, the resource is in fixed supply or can only generate a limited flow, as in the case of agricultural production, over exploitation can lead to its exhaustion when individuals do not take account of the overall consequences of their actions. This leads to what has been called "The Tragedy of the Commons" in [1].

In this paper we use a version of a model which was developed in the context of financial markets but we modify it to look at a problem of exhaustible resources, in particular that of fisheries. There is a substantial literature on fishing management which analyses the causes of over exploitation and the behaviour that leads to this. Much of that literature was based on understanding the strategies that individual boats use to decide when and where to fish. The simplest idea is that the individuals base their decisions on Catch per Unit Effort (CPUE), see [2]. This suggests that boats fish until their catch falls below a certain threshold and then move on. This is a purely individualistic model and argues that past individual experience is an adequate basis for decision making. Two questions arise here. Firstly, can one deduce the aggregate behaviour from the observed behaviour of individual vessels, and secondly, does the behaviour of other vessels influence the choices of a particular boat? The answer to the first question lies in the development of satellite technology which allows individual vessels to be identified and followed; this information provides a basis for analysing the individual and collective behaviour of fishing fleets. It is, of course, known that vessels do not act in total isolation and a model using tracking data for New Zealand fisheries was, for example, studied in Ref. [3]. This came to the conclusion that "there is evidence that vessels make decisions about where to fish based on both their own recent catch history and on observation about the location and aggregation of other vessels. There is no

* jose.moran@polytechnique.org

evidence that there is enough information transfer for vessels to make decisions on the basis of catch rates of the other vessels in the fleet". What was suggested was that while the influence of other players is taken into account, because of the limited information about the performance of other vessels it may not be the major driving influence for collective behaviour.

However, a more radical approach, abandoning a simple optimization approach had been developed earlier by Allen and McGlade [4]. They developed models in part based on the Lotka-Volterra equations which already incorporated recent advances in the understanding of the evolution of complex systems. They studied herd behaviour and simulations of a dynamic model of a Nova Scotia fishery. Their analysis revealed that human responses amplify rapid random fluctuations in recruitment and excite strong Lotka-Volterra type oscillations in a system that would normally settle to a stable stationary state. Their dynamic, multi-species, multi-fleet spatial model was calibrated to the Nova Scotian groundfish fisheries. They examined the role of "exploration" and "exploitation". They identified two types of hunters, "stochasts" or high-risk takers, and "cartesian" followers, or low risk takers. The result of the interaction between the two reveals, as they say, "the 'out of phase' relationship between abundance and the ease with which fishermen locate a highly sought species and its converse". They emphasize, contrary to more conventional analysis, "the importance of information exchange in defining the attractivity of a particular fishing zone to different fleets and the ability of the model to take into account coded information, misinformation, spying and lying; and the fact that models based on global principles, such as 'optimal efficiency' or 'maximum profit', are clearly of dubious relevance to the real world." The crucial difference between this and the work previously cited is that much more weight is given to information about the activity of others and the content of the messages about that activity is assumed to be much richer.

Our approach is in this spirit and is based on a model in which agents are "recruited" to a source of profit by those already benefiting from that source. The actors follow simple rules but their interaction can produce interesting dynamics. A related approach by computer scientists [5] suggested that the result might be that of a uniform distribution across the space in which the resource is found. We show that, depending on the weight given to the behaviour of others, vessels can typically operate near to their home port with occasional excursions to another area, but that changing the parameters of the model can lead to a persistent mixing of the two fleets with some boats from each area fishing in the other area. Since what is important is the probability that a boat follows others, the distribution of the boats over the two areas is determined by a stochastic process. This recalls a result of Allen and McGlade in which the survival of the fishery was dependent on the existence of some vessels which chose the place to fish at random and, as in many models of interaction, a degree of randomness may make an important contribution to the overall dynamics of the system.

The paper is organised as follows. In Section II, we present an overview of the data used in this article and introduce all relevant definitions. Section III introduces a model intended to reproduce the main stylized facts present in the data. The model is developed in Section IV using simplifying assumptions that are justified by numerical simulations. Finally, in Section V, we discuss further consequences of the model and in particular the different collective "phases" that describe the aggregate behaviour of fishing vessels.

II. EMPIRICAL FISHING DATA

As mentioned above, while applicable to a wider range of situations, our work was originally inspired by imitation and herding effects in fishing areas. Here we present the data we use together with some stylized facts, both quantitative and qualitative.

A. Description of the data

We use the Fishing Vessels Dataset from Global Fishing Watch [6] from Octobre 2012 to December 2016. Since our aim is to analyse the behaviour of fishermen seeking to exploit clearly distinguishable fishing areas, we geographically focus on the Adriatic Sea and specifically on the area encompassing the Italian cities of

Ancona and Pescara in which two of the largest fishing harbours and fish markets are situated (see for example [7] for a detailed study and description of the Ancona fishing market).[1] The two cities are separated by a reasonable distance of about 150 km, meaning that boats based in one city can easily find themselves fishing close to the other. Further, the existence of large and comparable fish markets in both cities hints at the possibility of matching fishing activity to market data, provided of course one has access to the latter. Note that while another city, San Benedetto del Tronto, lies between Ancona and Pescara, it is responsible for a rather negligible amount of the activity in the area.

We have also restricted our analysis to the behaviour of trawlers. These boats have a low cruise speed and fish in shallow waters close to the coast. A reasonable hypothesis, which we have confirmed with the local market authorities, is that trawlers fishing in the area are based in either one of the two cities and go out for a short amount of time before coming back to sell their catch on the local market. In particular we were told that, due to the policy of the market to sell fresh local fish, vessels (almost) always get back to the port after 24 hours. We were also told that while there is no ban for a boat registered in a given port to land their fish elsewhere, this seldom happens.[2] In other words, one expects trawlers based in, say, Pescara to leave port, fish for a day and then come back to sell their catch.

The reduced data set consists of daily tracking of these trawlers, identified by their 9-digit Maritime Mobile Service Identity (MMSI) number. Each vessel is tracked on a latitude-longitude grid with resolution 0.1.1 squared degrees. At Ancona and Pescara's latitude ($\approx 43^\circ$ North), this implies a spatial resolution of $\approx 11 \times 8$ km^2 (latitude by longitude). Finally, a preliminary study of the data shows that there is a significant reduction of fishing activity from Friday to Sunday, consistent with markets being open Monday through Thursday only. We have thus dropped the former from our data set, keeping only trading days to ensure significant fishing activity.

B. Defining fishing areas

To assign each trawler to its base port (Ancona or Pescara), we use the following heuristic procedure, which we then cross-validate with MMSI data provided by the Ancona market authorities. We introduce the notations:

- $h^i(x,t)$ the time spent by trawler i fishing at grid-point x on day t,
- $w^i(x) := \sum_t h^i(x,t) / \sum_{y,s} h^i(y,s)$, for the average fraction of time spent by trawler i fishing at point x,
- $d_{\mathrm{A}}(x)$ the distance between point x and Ancona, and d the distance between the two cities,
- $d^i_{\mathrm{A}} := \sum_x w^i(x) d_{\mathrm{A}}(x)$, the average distance separating trawler i and Ancona when it is fishing,
- $D^i_{\mathrm{A}} := \sum_x w^i(x) [d_{\mathrm{A}}(x)]^2$, the average square distance between trawler i and Ancona,

and of course symmetrically for Pescara with index P. We then define the neighborhood of Ancona and Pescara as the pseudo-ellipsoid with focal points the two ports, i.e. the set $\{x \mid d_{\mathrm{A}}(x)^2 + d_{\mathrm{P}}(x)^2 \leq 2d^2\}$, of course excluding land, see Fig. 1(c). We restrict our analysis to trawlers evolving within this area, namely $\{i \mid D^i_{\mathrm{A}} + D^i_{\mathrm{P}} \leq 2d^2\}$. We then assign the trawlers to one of the two ports according to their average distance to each of them. Defining two distinct areas as:

$$\mathscr{D}_{\mathrm{A}} = \left\{x \mid d_{\mathrm{A}}(x) \leq d_{\mathrm{P}}(x) \quad \text{and} \quad d_{\mathrm{A}}(x)^2 + d_{\mathrm{P}}(x)^2 \leq 2d^2\right\} \tag{1a}$$

$$\mathscr{D}_{\mathrm{P}} = \left\{x \mid d_{\mathrm{P}}(x) < d_{\mathrm{A}}(x) \quad \text{and} \quad d_{\mathrm{A}}(x)^2 + d_{\mathrm{P}}(x)^2 \leq 2d^2\right\}, \tag{1b}$$

a given trawler is assigned to, say, Pescara if its fishing time-weighted average position lies in $\mathscr{D}_{\mathrm{P}}$. In other words $i \in$ Pescara (resp. Ancona) if $d^i_{\mathrm{P}} \leq d^i_{\mathrm{A}}$ (resp. $d^i_{\mathrm{A}} < d^i_{\mathrm{P}}$). To validate our method of home port identification, we

[1] Note that with this publicly available database, our analysis can be reproduced in any other place of the world where two competing harbours lie reasonably close to each other.

[2] According to the director of the Ancona fish market, there are no relationships with nearby wholesale markets (Pescara and San Benedetto del Tronto), and, two or three times a year, it happens that a boat based in the nearby port in the north (Fano or Cattolica) comes to sell.

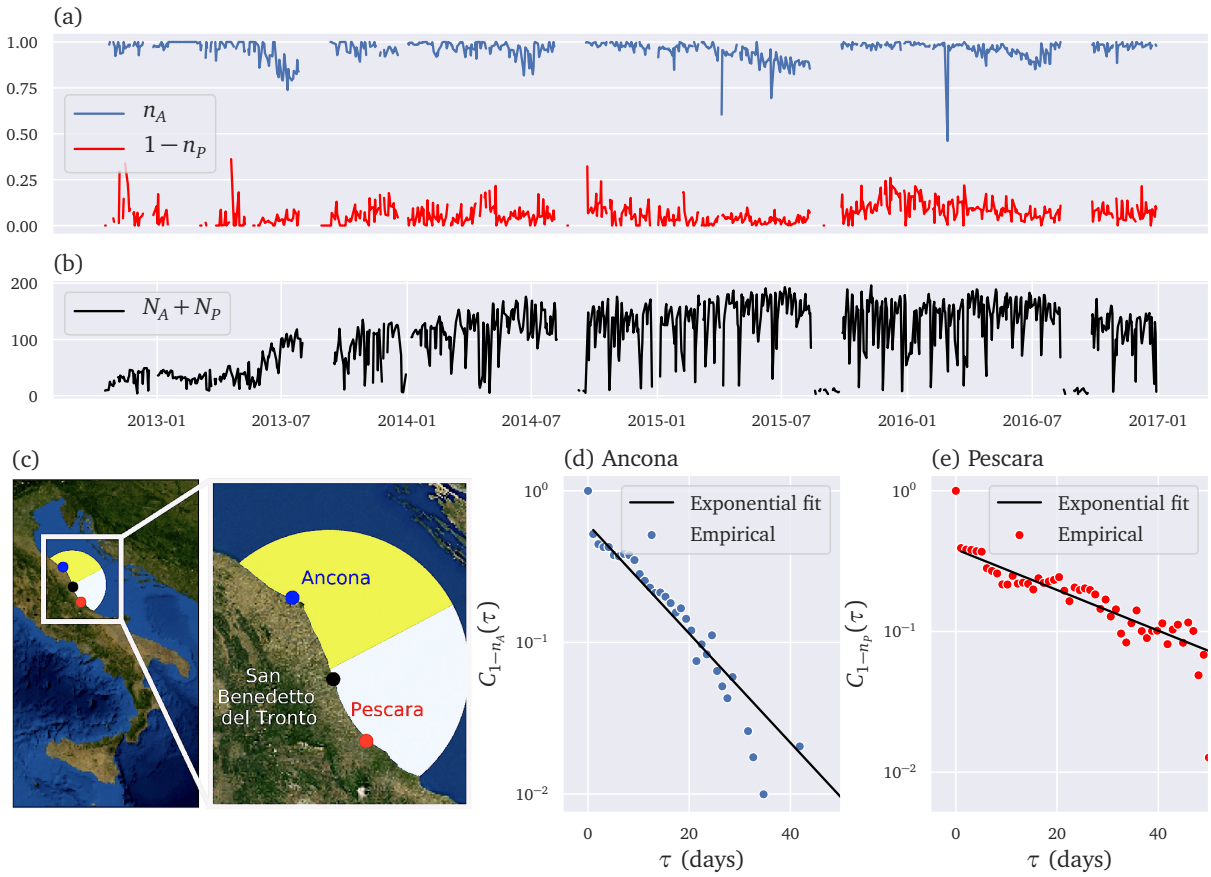

FIG. 1. Description of empirical data. Blue curves and markers correspond to data related to the area of Ancona, while red curves and markers correspond to Pescara. (a) Plot of the fractions $n_i(t)$, as defined in Eq. (2) (b) Plot of the total number of active boats through time $N_A + N_P$. (c) Satellite view of the Adriatic Sea along with the areas $\mathscr{D}_\mathrm{A}$ and $\mathscr{D}_\mathrm{P}$, as defined in Eq. (1). (d) and (e) Autocorrelation functions $C_{1-n_i}(\tau)$, as defined in Eq. (3) for both zones. For Ancona we find an exponential fit with a decay rate of ≈ 11 days, while for Pescara we find a decay of ≈ 33 days.

were able confront our classification to the list of the Ancona-based trawlers, kindly provided by the Ancona fish market authorities. Up to a few minor errors, notably related to having identified as Ancona-based a few vessels based in the much smaller San Benedetto del Tronto, the cross-check was successful. Over the whole period we counted $N_\mathrm{A} = 108$ Ancona-based trawlers and $N_\mathrm{P} = 118$ Pescara-based trawlers.

C. Stylized facts

Having tagged each boat to either Ancona or Pescara, we now turn to studying the dynamics of fishing within the two areas $\mathscr{D}_\mathrm{A}$ and $\mathscr{D}_\mathrm{P}$. We define the fraction $n_\mathrm{A}(t)$ of time spent by Ancona-based vessels fishing in $\mathscr{D}_\mathrm{A}$ namely:

$$n_\mathrm{A}(t) = \frac{\sum_{x\in\mathscr{D}_\mathrm{A}, i\in\mathrm{Ancona}} h^i(x,t)}{\sum_{y, i\in\mathrm{Ancona}} h^i(y,t)}, \tag{2}$$

and vice-versa $n_\mathrm{P}(t)$ for Pescara. Figure 1(b) displays the evolution of $n_\mathrm{A}(t)$ and $n_\mathrm{B}(t)$ throughout the period of interest. While these fractions are most often very close to 1, indicating as one would intuitively expect

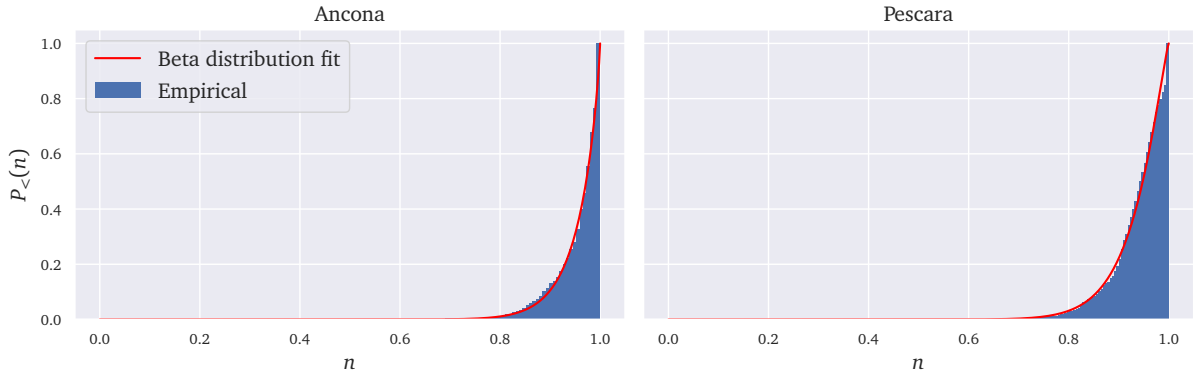

FIG. 2. Cumulative distribution function (cdf) of the fractions n_A and n_P as defined in Eq. (2). The solid red curves correspond to a fit with a generalized Beta distribution, which has a cdf given by $P_>(n) = C\int_0^n \mathrm{d}x\; x^{\gamma_0-1}(1-x)^{\gamma_1-1}$ with C a normalization constant. The parameters for Ancona are $\gamma_0 = 18.48$ and $\gamma_1 = 0.82$, while those for Pescara read $\gamma_0 = 17.73$ and $\gamma_1 = 1.27$.

that trawlers spend most of their time fishing near their home port, one can see, however, that they regularly undergo persistent excursions, revealing that a sizeable fraction of the vessels in each area decide collectively to go elsewhere.

To evaluate the typical length of such excursions, Figs. 1 (d) and (e) display the auto-correlation functions:

$$C_{1-n}(\tau) := \mathrm{Cor}\left(1-n(t+\tau), 1-n(t)\right), \tag{3}$$

for both $n_A(t)$ and $n_P(t)$. These are well fitted by the sum of a delta-peak at 0, which can be attributed to measurement noise and other exogenous factors such as the weather, and an exponentially decaying function with typical timescale ranging from ≈ 11 to ≈ 30 days. Interestingly enough, Fig. 2 reveals that the empirical distributions of n_A and n_P are remarkably well fitted by a Beta distribution. This is exactly what one obtains in Kirman and Föllmer's ant recruitment model [8, 9], in which the Beta distribution emerges as the stationary distribution describing a colony of ants preying on two distinct food sources. Such a distribution also emerges as the stationary distribution describing genetic populations between two competing alleles [10, 11]. The key ingredient in these models is the competition between two different entities, be they food sources or genetic alleles. In Kirman and Föllmer's ant model however, the two food sources are strictly equivalent and the resulting Beta distribution describing the fraction of ants at each source is necessarily symmetric, at odds with the results obtained in the present setting. This motivates the asymmetric zones model introduced below. Another significant difference with Kirman and Föllmer's original model is that the "food sources" here are not inexhaustible, as fish cannot reproduce at an infinite rate.

These empirical results and observations motivate us to introduce a model extending Kirman and Föllmer's original ant recruitment model to our context. In essence, one can think of the two cities as two distinct ant colonies that can obtain their food from either of the two zones. For each colony, the further fishing area is necessarily less attractive, leading to the asymmetric character of the distribution. In addition, not being in a setting with unlimited resources, our model should take into account the fact that over-fishing may deplete the sea.

III. A SIMPLE MODEL

Kirman and Föllmer's original ant-recruitment model [8] was successful at explaining a rather puzzling fact well known to entomologists [12, 13]. Ants, faced with two identical and inexhaustible food sources tend

to concentrate on one of them and occasionally switch to the other. Such intermittent herding behaviour is observed in a variety of settings including choosing between equivalent restaurants [14], or financial markets [15–17] consistent with large endogenous fluctuations. In the model, at each time step a given ant may either (i) encounter another ant from the other inexhaustible food source and decide to switch to her peer's source (be recruited), or (ii) spontaneously decide to switch food sources without interacting. The driving mechanism of the dynamics results from the trade-off between the intensity of the noise-term ε (spontaneous switching), and that of the interaction term μ, see also [9].

Here we present an extension of Kirman and Föllmer's original model to account for *exhaustible* and asymmetric sources, notably aimed at accounting for some of the stylized facts presented in the previous section for fishing areas. Seeking to model fishermen exploiting a set of fishing areas, we imagine that boats follow the same basic dynamics as the ants: if they initially fish within a certain zone, they may decide to move elsewhere either because they see their peers fishing there, deciding to imitate them because they assume that their yield is good, or spontaneously decide to move elsewhere randomly for the sake of exploration.

As discussed above, our model has two major differences that depart from the original ant-recruitment model. First, we consider that a fishing area has finite resources: fish reproduce until reaching a certain finite capacity but they are also depleted by fishermen in the area (as in e.g. MacArthur's models [18, 19]). As a consequence, we assume that the random switching rate at which fishermen decide to depart from a given area depends on the fish population of that area. Note that this is very close in spirit to the modelling done in Ref. [4], albeit that our model takes into account imitative behaviour in fishermen. The second difference with the ant model is that we imagine two "colonies" instead of just one, corresponding to vessels based at the two different fishing ports of Ancona and Pescara. Guided by the idea that fishermen prefer to go to areas close to their own home port, notably to save fuel, we introduce an asymmetry between the fishing areas for each food source.

The two ports, labelled A and P, have two distinct populations of fishermen, which may decide to exploit two fishing areas, S_1 and S_2, with the fishermen from A preferring to fish at S_1 and vice versa. One may of course reasonably argue that this view is far too coarse-grained, and that there may be, for example, many different fishing areas that are available close to each port. It is however possible to show under mild hypotheses that the two zones S_1 and S_2 in the model can be seen as the aggregation of a large number of smaller areas, with the same dynamics, see Appendix B for details. For clarity, we shall define the model in discrete time, before moving into continuous time for analytical convenience.

Without loss of generality, we focus only on the dynamics of fishing vessels at one of the two ports, say Ancona, as we assume that fishermen only interact with boats coming from the same city.[3] We define now N_A and N_P as the number of boats based at Ancona and Pescara respectively, and let each of them decide to go to any of the two areas S_1 and S_2. We denote $m_i(t)$, with $i = 1, 2$, their respective fish populations at time t, and further assume that:

- Boats only fish in one area each day (consistent with discussions with port authorities) and come back to that area if they don't decide to switch to another one for the next day.
- A vessel's daily catch $c_i(t)$ is proportional to the amount of fish available in the area: $c_i(t) = \frac{\beta}{N_A} m_i(t)$ with $\beta/N_A \in [0; 1]$.[4]
- Fish reproduce at a multiplicative rate ν_i, which we take to be equal to ν for both areas.
- As a first approximation, fish do not travel from one area to the other.[5]
- The fish population within any area cannot exceed a carrying capacity K_i, which is the maximal population that can be present within an area in the absence of fishing. This carrying capacity is the same for all areas, as we have taken all of them to be equivalent. Without loss of generality, we take $K_1 = K_2 = 1$ in all that follows.

[3] Anecdotal evidence suggests indeed that the main interaction between people working in different boats happens at port in the fishing market or during informal conversation.

[4] Without changing our main conclusions, one could also allow for noise by drawing $c_i(t)$ from a given distribution centred about $\beta m_i(t)/N$. This would allow us to introduce randomness into the fishing efficiency of each trawler, an interesting extension that we leave for further work.

[5] This constraint can be easily relaxed by e.g. adding a migration term where fish from 2 move to 1 at a certain rate and vice-versa. In practice, this would only tend to prevent the difference between the two fish populations from fluctuating too wildly.

Note that these definitions, which also amount to thinking of the fish population as consisting of the same species in both areas, are partially justified by our considering only trawlers, that therefore fish only very specific, shallow water dwelling species.

We further define $N_{\mathrm{A},i}(t)$ the number of vessels from port A fishing at zone i at time t (and $N_{\mathrm{P},i}(t)$ respectively). The number of fishing vessels in each port is fixed, implying for all t: $N_{\mathrm{A},1}(t)+N_{\mathrm{A},2}(t)=N_{\mathrm{A}}$. Our assumptions translate into following evolution for the fish population:

$$m_i(t+1)-m_i(t)=m_i(t)\big[\nu g(m_i(t))-\beta\left(N_{\mathrm{A},i}(t)+N_{\mathrm{P},i}(t)\right)\big], \tag{4}$$

where the function g must satisfy $g(0)=1$ and $g(1)=0$.

On the right hand side, the first term $\nu m_i g(m_i(t))$ models the amount of fish that are born between t and $t+1$ in absence of fishing; it is given by a birth-rate ν when the fish aren't too plentiful, but goes to 0 as the zone gets saturated and cannot sustain any more fish. The simplest assumption one can make is that of logistic growth, leading to $g(m_i(t))=1-m_i(t)$. It follows that $m_i(t)\in[0;1],\ \forall t$, where $m=1$ corresponds to a fishing area at full capacity and $m=0$ corresponds to a depleted area. Under these assumptions, the evolution of the fish population is of the Lotka-Volterra type, as advocated in [4].[6] The second term on the right hand side corresponds simply to the decrease in fish population because of fishing activity.

Furthermore, we assume that a fishing vessel based at A fishing at i can randomly decide to go elsewhere with probability $\varepsilon_{\mathrm{A},i}f(m_i(t))$, where the function f satisfies $f(1)=1$ and $f(0)=1+\kappa$. Here, $\varepsilon_{\mathrm{A},i}$ controls the base intensity of the noise, that can take a maximal value $\varepsilon_{\mathrm{A},i}(1+\kappa)$ when the zone is depleted. Fishermen have then a higher incentive to go elsewhere as their fishing yield decreases, and we highlight the preference of fishermen from A for zone 1 by setting $\varepsilon:=\varepsilon_{\mathrm{A},1}=\varepsilon_{\mathrm{A},2}/C_\varepsilon$ with $C_\varepsilon>1$ a parameter controlling the degree of asymmetry between zones S_1 and S_2 for a fisher from A. This allows us to have a higher spontaneous switching rate $S_2\to S_1$ for fishermen from A.

Besides this random switching rate, we add in the crucial element in our model, which is that agents imitate each other. Each day, a fisherman randomly picks one of his peers and decides to imitate him with probability μ/N, so that μ is the average fraction of boats deciding to take an imitation strategy at each step. In this case, the probability that a boat from A initially at zone S_i decides to move to zone S_j is given by:

$$P_{\mathrm{A}}(S_i\to S_j)=\varepsilon_{\mathrm{A},i}f(m_i(t))+\frac{\mu}{N_{\mathrm{A}}}\frac{N_{\mathrm{A},j}(t)}{N_{\mathrm{A}}-1}. \tag{5}$$

Writing then $n_{\mathrm{A},i}=N_{\mathrm{A},i}/N_{\mathrm{A}}$, we take the limit $N_{\mathrm{A}},N_{\mathrm{P}}\to\infty$ with $N_P/N_{\mathrm{A}}=C_N$ fixed. Within this limit, we denote $\mathbf{n}_A=(n_{\mathrm{A},1},n_{\mathrm{A},2})$ and $\mathbf{m}=(m_1,m_2)$ and study the probability density $\rho(\mathbf{n}_{\mathrm{A}},\mathbf{n}_{\mathrm{P}},\mathbf{m})$ of all the variables of the model. The equation one obtains is called the Fokker-Planck equation [21], also known as the Kolmogorov forward equation in applied mathematics and closely related to the Hamilton-Jacobi-Bellman equations describing the optimal choice of a rational agent; it can be interpreted as the continuous limit of a Markovian transition matrix. In the case of our model, the Fokker-Planck equation reads:

$$\begin{aligned}\partial_t\rho=&-\varepsilon\partial_{n_{\mathrm{A},1}}\left[C_\varepsilon f(m_2)-n_{\mathrm{A},1}\left[C_\varepsilon f(m_2)+f(m_1)\right]\right]\rho+\mu\partial^2_{n_{\mathrm{A},1},n_{\mathrm{A},1}}\left[n_{\mathrm{A},1}(1-n_{\mathrm{A},1})\right]\rho+\left[(n_{\mathrm{A},1},m_1)\leftrightarrow(n_{\mathrm{P},2},m_2)\right]\\&-\partial_{m_1}\left[\nu(1-m_1)-\beta\left(n_{\mathrm{A},1}+C_N(1-n_{\mathrm{P},2})\right)\right]m_1\rho+\left[(m_1,n_{\mathrm{A},1},n_{\mathrm{P},2})\leftrightarrow(m_2,1-n_{\mathrm{A},1},1-n_{\mathrm{P},2})\right],\end{aligned} \tag{6}$$

where the bracket $[x\leftrightarrow y]$ is shorthand for the same expression where one replaces x by y.

These equations fully close the model, which in our view represent the simplest setting for a system with limited resources exploited by entities with a myopic exploration/imitation strategy. As they stand, however, they cannot be solved analytically. We shall now resort to a mean-field approximation to find a solution.

[6] As an interesting anecdote, we learned in [20] that "Vito Volterra was born in the Jewish ghetto of Ancona in 1860, shortly before the unification of Italy, when the city still belonged to the Papal States", and that "in 1925, at age 65, Volterra became interested in a study by the zoologist Umberto D'Ancona, who would later become his son-in-law, on the proportion of cartilaginous fish (such as sharks and rays) landed in the fishery during the years 1905–1923 in three harbours of the Adriatic Sea: Trieste, Fiume and Venice. D'Ancona had noticed that the proportion of these fish had increased during the First World War, when the fishing effort had been reduced". This led him to take interest in models that Alfred Lotka had first used to model very general population dynamics, and that we now apply, without knowing any of this at first, to the fish population dynamics at the ports of Ancona and Pescara.

IV. MEAN-FIELD APPROXIMATION

Solving the Fokker-Planck equation (6) is a very difficult task, as the different terms that intervene take into account the interactions between the proportion of fishermen in a given zone and the fish population in it. In general, these two quantities fluctuate in time, and the main difficulty lies in unravelling how these fluctuations interact. However, if one is interested in a very aggregated picture, one can simplify the problem significantly by calculating the behaviour of the fish *as if* they were only subject to the averaged, fluctuation-free, action of the fishing boats and vice-versa. This is what is known as the *mean-field approximation*, which allows to replace, as a first step, the behaviour of the fish populations m_i with their long-time averages. Taking Eq. (4) in the continuous time limit, the evolution of the fish population of, e.g., zone 1 follows:

$$\frac{\mathrm{d}m_1}{\mathrm{d}t} = m_1(t)\big(\nu(1-m_1(t)) - \beta\left(n_{\mathrm{A},1} + C_N\left(1-n_{\mathrm{P},2}\right)\right)\big). \tag{7}$$

If we take the average of this equation, we expect the left hand side to be $\frac{\mathrm{d}\mathbb{E}[m_1]}{\mathrm{d}t} = 0$ as the average is not expected to fluctuate in time.[7] This yields the following expression for the right hand side:

$$\mathbb{E}[m_1] = \left[1 - \frac{\beta}{\nu}\left(\mathbb{E}\left[n_{\mathrm{A},1}\right] + C_N\left(1-\mathbb{E}\left[n_{\mathrm{P},2}\right]\right)\right)\right]_+, \tag{8}$$

where $[x]_+ = x\mathbf{1}_{x>0}$ denotes the positive part of x. In particular, one can see that there exists a trivial extinction line for the fish population for:

$$\nu = \beta\left[\mathbb{E}\left[n_{\mathrm{A},1}\right] + C_N\left(1-\mathbb{E}\left[n_{\mathrm{P},2}\right]\right)\right], \tag{9}$$

which corresponds to the case where the reproductive rate of fish corresponds exactly to the rate at which they are fished.

We now do the same mean-field approximation the other way around to simplify the evolution of the fishermen. We insert Eq. (8) into the vessels' dynamics by replacing the argument of $f(m_i)$ by the average, as $f(\mathbb{E}[m_i]) := f_i$, which amounts to saying that the boats only interact with the average behaviour of the fish. Choosing, to be precise, a linear function for f, i.e. $f(x) = 1+\kappa(1-x)$, the average $\mathbb{E}\left[n_{\mathrm{A},1}\right]$ can now be easily computed from Eq. (6) by setting the drift term to 0, as:

$$\mathbb{E}\left[n_{\mathrm{A},1}\right] = \frac{C_\varepsilon f_2}{C_\varepsilon f_2 + f_1} = \frac{C_\varepsilon\left(1+\kappa(1-\mathbb{E}[m_2])\right)}{2+\kappa\left[1-\mathbb{E}[m_1] + C_\varepsilon\left(1-\mathbb{E}[m_2]\right)\right]}. \tag{10}$$

Therefore, the mean-field approximation applied to the quantities m_1 and n_{A} have allowed to derive the two Eqs. (8) and (10), and therefore to obtain self-consistently the averages of these quantities. The next step is to obtain a fuller picture of the aggregate behaviour of the vessels within the mean-field approximation, and to obtain for example the probability density associated with it.

A. Stationary solutions

Consistent with our mean-field approximation, we set $m_1 = \mathbb{E}[m_1]$ (resp. $m_2 = \mathbb{E}[m_2]$) in Eq. (6) to obtain a Fokker-Planck equation that describes the vessels. In the previous equation, vessels from the two ports interacted indirectly through fishing in the same zone and depleting the fish in it, motivating all the boats in

[7] This average is taken with respect to infinitely many possible realizations of the stochastic process describing the evolution of our model. Nonetheless, because the model is ergodic we expect that this averaging is also true when one considers time-averages, meaning that we take a single realization of the process and look at the average of m_1 in time.

that zone to leave. Replacing the behaviour of the fish by its average amounts to neglecting this effect, and to an effective decoupling of the two variables n_{A} and n_{P}, as:

$$\partial_t \rho = \partial_{n_{\mathrm{A},1}} J_1 + \partial_{n_{\mathrm{P},2}} J_2, \tag{11}$$

where:

$$J_1 = -\varepsilon \left[C_\varepsilon f_2 - n_{\mathrm{A},1} \left[C_\varepsilon f_2 + f_1 \right] \right] \rho + \mu \partial_{n_{\mathrm{A},1}} \left[n_{\mathrm{A},1} (1 - n_{\mathrm{A},1}) \right] \rho, \tag{12}$$

and where the transposition to find the definition of J_2 is transparent. The two quantities J_1 and J_2 are probability fluxes, and for example $J_1\left(n_{\mathrm{A},1}, t\right)$ can be interpreted as the probability mass going from $n_{\mathrm{A},1} + \Delta n$ to $n_{\mathrm{A},1}$ for an infinitesimal Δn during an infinitesimal amount of time.

The stationary state is found by setting $J_1 = 0$ and $J_2 = 0$, meaning that there is no probability flux in the model, and solving the obtained equations for ρ. The decoupling of the two variables $n_{\mathrm{A},1}$ and $n_{\mathrm{P},2}$ allows one to write the density as the product of two independent densities, as

$$\rho(n_{\mathrm{A},1}, n_{\mathrm{P},2}) = \rho_1\left(n_{\mathrm{A},1}\right) \rho_2\left(n_{\mathrm{P},2}\right), \tag{13}$$

with:

$$\rho_1(n_{\mathrm{A},1}) = C_1 n_{\mathrm{A},1}^{\gamma_{\mathrm{A},0}-1} \left(1 - n_{\mathrm{A},1}\right)^{\gamma_{\mathrm{A},1}-1}, \quad \rho_2\left(n_{\mathrm{P},2}\right) = C_2 n_{\mathrm{P},2}^{\gamma_{\mathrm{P},0}-1} \left(1 - n_{\mathrm{P},2}\right)^{\gamma_{\mathrm{P},1}-1}, \tag{14}$$

where C_1 and C_2 are normalisation constants and the γ parameters for the ρ_1 distribution (the parameters for ρ_2 can be easily deduced) read:

$$\gamma_{\mathrm{A},0} = \frac{\varepsilon}{\mu} C_\varepsilon f_2, \quad \gamma_{\mathrm{A},1} = \frac{\varepsilon}{\mu} f_1. \tag{15}$$

Note also that full dynamical solutions $\rho(n_{\mathrm{A},1}, t)$, $\rho(n_{\mathrm{P},2}, t)$ can be obtained in terms of hypergeometric functions, in the same spirit as [9], see Appendix A.

For the reader unfamiliar with Fokker-Planck equations and stochastic processes, the following thought experiment may help in understanding what we've stated mathematically above. The model in Sec. III can be run as a computer simulation where $n_{\mathrm{A},1}$ and $n_{\mathrm{P},2}$ correspond to numbers between 0 and 1 and can be known at all times. It is then possible to run a very large number of simulations with the same initial conditions for these two variables and to compute cross-sectional histograms for these variables at a given time-point, that is the histograms of the same variable at the same time but through different simulations. The Fokker-Planck equation describes how these histograms will change in time, before eventually settling onto distributions described by Eq. (14). The model is however ergodic, and if we also take one single simulation and run it for a very long time, we can plot the histogram of, say, $n_{\mathrm{A},1}(\{t_i\})$ at randomly sampled times t_i and we will observe a histogram described by the density $\rho_1(n_{\mathrm{A},1})$.

Our model thus replicates successfully the observed distributions shown in Fig. 2, and captures the qualitative behaviour from Fig. 1. An example of numerical simulation of the model is provided in Fig. 3. For this Figure, we have set $\mu = 1$ as it only amounts to a certain choice of the timescale, while picking a small value $\kappa = 0.1$ to keep $f_2, f_1 \approx 1$. We have then picked ε and C_ε such as to match the values for γ_0 and γ_1 from Fig. 2.

B. Dynamics and correlation functions

Within the mean-field model above, it is straightforward to show using tools from stochastic calculus (see the appendices in Ref [9]) that the variable $n_{\mathrm{A},1}$ follows a stochastic differential equation:

$$\frac{\mathrm{d}n_{\mathrm{A},1}}{\mathrm{d}t} = \mu \left(\gamma_{\mathrm{A},0} - \left(\gamma_{\mathrm{A},0} + \gamma_{\mathrm{A},1} \right) n_{\mathrm{A},1} \right) + \sqrt{2\mu n_{\mathrm{A},1} \left(1 - n_{\mathrm{A},1}\right)} \eta(t), \tag{16}$$

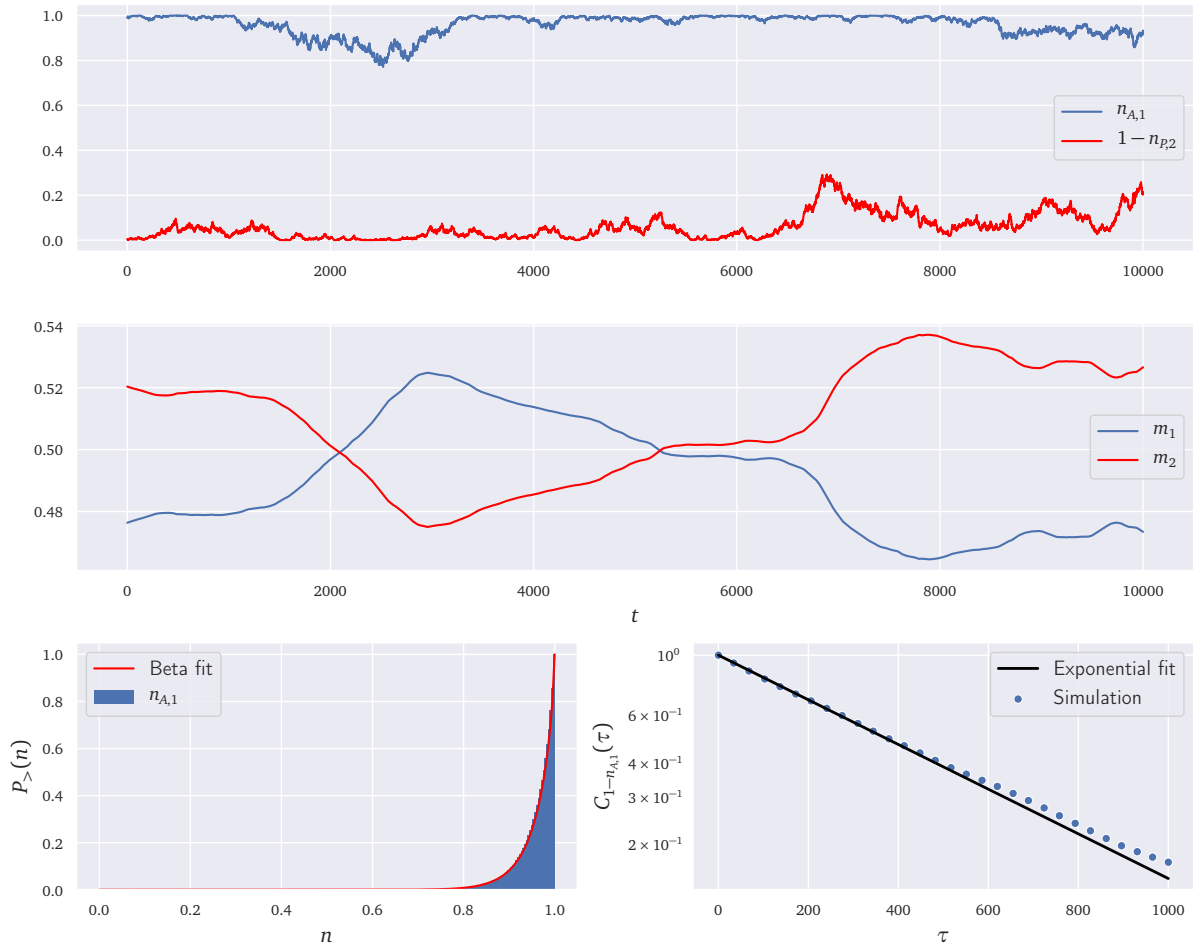

FIG. 3. Numerical simulation of our model. We have chosen the different parameters to obtain the same stationary Beta distribution as that observed in Fig. 2. Note also the similarity of the Figure on the left with plot (a) in Figure 1. We have used the parameters $\varepsilon = 0.69$, $\nu = 10$, $\beta = 5$, $C_N = 1$, $C_\varepsilon = 26.5$ for Ancona and 15.7 for Pescara and $\kappa = 0.1$. The upper panel shows two trajectories $n_{\mathrm{A},1}(t)$ and $n_{\mathrm{P},2}(t)$. The middle panel shows the fish populations $m_1(t)$ and $m_2(t)$. The bottom left panel shows the cumulative density function for $n_{\mathrm{A},1}$ along with a Beta distribution fit. The bottom right panel shows the empirical correlation function as defined by Eq. (17) along with an exponential fit. Note that the fish populations oscillate around the theoretical mean-field value $m = 0.5$, and that large oscillations coincide with large collective movements of the fishermen in both areas.

with η a gaussian white noise of unit variance. This equation may be solved formally by integration, just as one would for a standard ordinary differential equation. With this formal solution, it is then possible to compute the auto-correlation of $1-n_{\mathrm{A},1}$, defined as in Eq. (3), to find

$$C_{1-n_{\mathrm{A},1}}(\tau) = \exp\left(-\mu\left(\gamma_{\mathrm{A},0} + \gamma_{\mathrm{A},1}\right)\tau\right), \tag{17}$$

which is exactly what one sees from the data in Fig. 1 (d) and (e), provided one interprets the delta-peak at $\tau = 0$ as the result of exogenous noise, e.g. weather conditions. Indeed if one considers that the measured signal is, in fact, a noisy signal,

$$\tilde{n}(t) = (1-\sigma)n(t) + \sigma\xi(t), \tag{18}$$

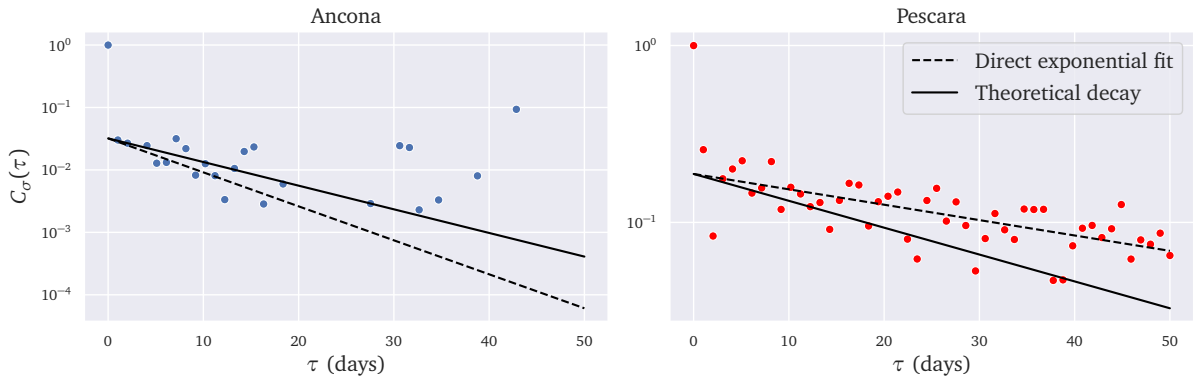

FIG. 4. Empirical correlation function $C_\sigma(\tau)$ as defined in Eqs. (20) and (21). The solid black line is the theoretical prediction given the estimations of γ_0 and γ_1 from the empirical probability distribution in Fig. 2 and from the subsequent estimation of μ using the exponential decay factor from Fig. 1. The reliable computation of σ depends of course on the proper estimation of these parameters, and we expect them to be noisy. Nonetheless, the agreement with theory, especially in the case of Pescara, is rather good.

where $n(t)$ is the "true" process and $\xi(t)$ is a gaussian white noise of unit variance, then one can show directly that the measured correlation function reads:

$$C_{1-\tilde{n}}(\tau) = \delta(\tau) + \frac{(1-\sigma)^2}{\sigma^2} C_{1-n}(\tau). \tag{19}$$

We have checked that the correlation function given in Eq. (17) agrees with our numerical simulations as well; the results are shown in the bottom right panel in Fig. 3.

The agreement is excellent both between the mean-field theory and the data, indicating that our model can correctly replicate the main dynamical features of real data from fishing dynamics. Furthermore, one can deduce the value of μ from the values of γ_0, γ_1 and the decay factor in the exponential, that should match $\mu(\gamma_0+\gamma_1)$. Using this formula, we find $\mu = 4.3\cdot 10^{-3}$ for Ancona and $\mu = 1.7\cdot 10^{-3}$ for Pescara.

Note that the middle panel in Fig. 3 shows very interesting dynamics, with the fish population oscillating about its average value $\mathbb{E}[m_1] = \mathbb{E}[m_2] = 0.5$ through visible interactions with the amount of boats fishing in the two areas. Note for example that the fish population tends to increase when the boats leave an area, but this is detrimental to the fish in the other area. In the Figure, it is also visible that boats from Pescara arriving at $t \approx 7000$ arriving in the zone close to Ancona had a detrimental effect to the population m_1 of fish close to Ancona, and the population in that zone did not necessarily have the time to recover from that excess in the time allowed by the simulation.

More complicated correlation functions can also be computed, along the lines of [9], although they are more prone to statistical noise. For example, using using the techniques described in detail in Ref. [9], one can show that the polynomial defined by:

$$\sigma_{\mathrm{A}}(n_{\mathrm{A},1}) = n_{\mathrm{A},1}^2 - \frac{2(\gamma_{\mathrm{A},0}+1)}{\gamma_{\mathrm{A},0}+\gamma_{\mathrm{A},1}+2} n_{\mathrm{A},1}, \tag{20}$$

has an autocorrelation function that is exponential, meaning that $C_{\sigma_A}(\tau) = \mathrm{Cor}\left(\sigma_{\mathrm{A}}\left(n_{\mathrm{A},1}(t+\tau)\right), \sigma_{\mathrm{A}}\left(n_{\mathrm{A},1}(t)\right)\right)$ verifies:

$$C_{\sigma_{\mathrm{A}}}(\tau) = \exp\left(-2\mu(1+\gamma_{\mathrm{A},0}+\gamma_{\mathrm{A},0})\,\tau\right), \tag{21}$$

and the same can of course be transposed to the variables indexed by P.

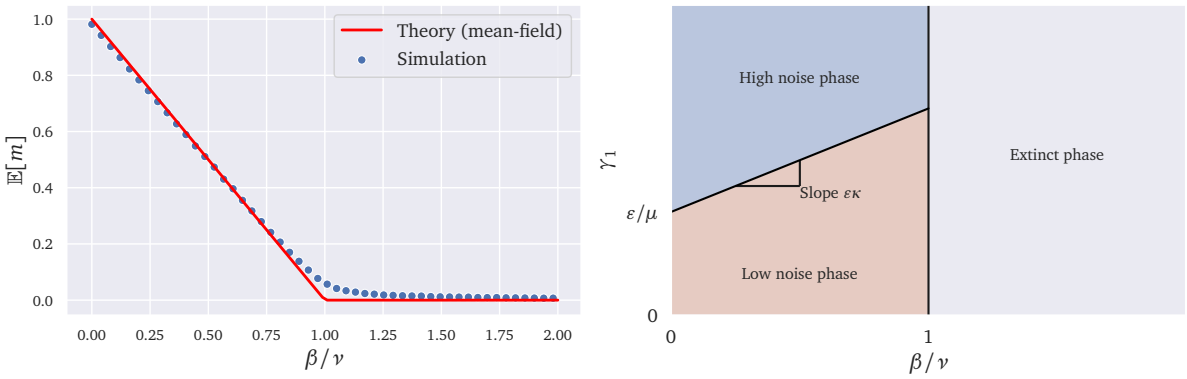

FIG. 5. Left: Numercial results (same parameters as in Figs 3 and 4). The simulation was run for $T = 10^5$ steps and with $\nu = 10$. Note that the convergence of the simulation to the mean-field results from Eq. (23) improves as T or ν grow larger. Right: Phase diagram of the model. Note that the high/low noise frontier line could be extended in the extinct phase; indeed, without further ingredients, in the extinct phase boats move between the two areas as in the non-extinct phase even though they are not able to fish anymore.

We have tested this prediction in Fig. 4. This correlator is necessarily more affected by measurement noise, because it is of order two in the n variables and because it depends on a reliable estimation of the γ and μ variables. Considering these limitations, the theoretical prediction is rather satisfactory when compared with the data, especially in the case of Pescara.

V. THE SYMMETRIC LIMIT

In general, the fixed point equations defined at the beginning of Section IV linking the averages $\mathbb{E}[m_i]$ with the averages $\mathbb{E}[n_i]$ cannot be solved directly. Nonetheless, if one takes $C_N = 1$ to have two fishing areas that are perfectly symmetric, then the equations simplify considerably as this immediately implies $f_1 = f_2$, with Eq. (10) becoming:

$$\mathbb{E}\left[n_{\mathrm{A},1}\right] = \mathbb{E}\left[n_{\mathrm{P},2}\right] = \frac{C_\varepsilon}{C_\varepsilon + 1}. \tag{22}$$

One can then write Eq. (8) more explicitly, to obtain the following extinction line:

$$\mathbb{E}[m_1] = \mathbb{E}[m_2] = \begin{cases} 1 - \frac{\beta}{\nu} & \text{if} \quad \beta < \nu \\ 0 & \text{if} \quad \beta \geq \nu, \end{cases} \tag{23}$$

which has the intuitive interpretation that the population within a given area goes extinct if the fishing rate is larger than the reproduction rate of fish in the area. Figure 5 shows that the agreement of numerical simulations with our mean-field analysis is excellent. One should note however that convergence may be slow when $\nu \to 0$, as this parameter controls the global fish population typical timescale.

Note also that in this case, one can directly compute $f_1 = f_2 = 1 + \frac{\kappa\beta}{\nu}$. The parameters in Eq. (15) simplify to yield:

$$\gamma_0 = \frac{\tilde{\varepsilon}}{\mu} C_\varepsilon, \quad \gamma_1 = \frac{\tilde{\varepsilon}}{\mu}, \tag{24}$$

where we've dropped the A index as the parameters for both areas A and P are identical, and where we've set $\tilde{\varepsilon} := \varepsilon\left(1 + \frac{\kappa\beta}{\nu}\right)$.

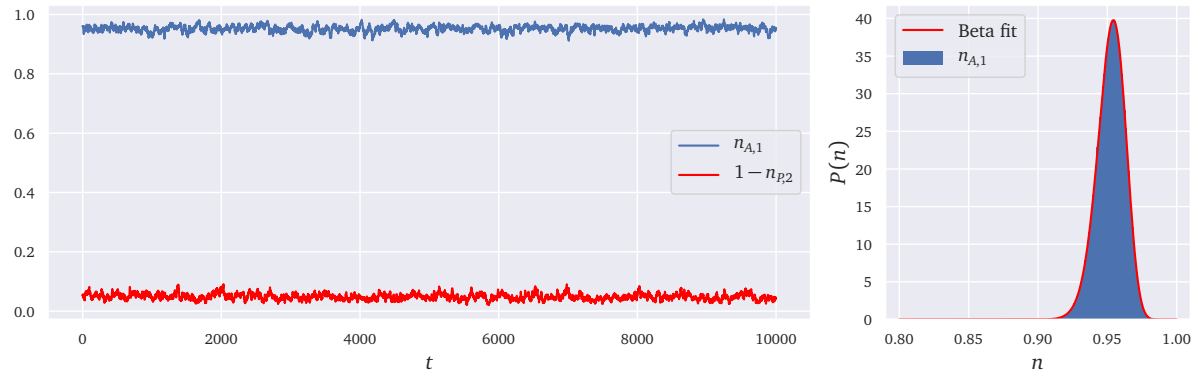

FIG. 6. Numerical simulations in the case $\gamma_1 > 1$. The parameters are the same as that of Fig. 3, but with $\kappa = 10$ instead. The Beta fit is compatible with the predicted theoretical values from Eq. (24). Note that, in contrast with Fig. 2, we show the probability density instead of the cumulative density function.

In this limit it is very clear that our mean-field model amounts to a modification of the original ant model [8], where the noise ε is augmented because of the sensitivity of the fishermen to the local fish population by the factor given above, and where we have introduced an asymmetry between the two areas/food-sources through the parameter C_ε.

One would then typically expect to have always have $\gamma_0 > 1$ because of the strong preference for the fishing area closest to one's home port. However, if ε or κ are strong enough, one can have a crossover at $\gamma_1 = 1$, separating a regime where the boats are all frequently found to be close to their home port, corresponding to $\gamma = 1$ and $n_{\mathrm{A},1} = 1$ as the most probable value in the distribution, from a regime where there is mixing and the most probable value is $n_{\mathrm{A},1} < 1$, corresponding to $\gamma_1 > 1$.

The simulations displayed in Fig. 3 correspond to $\gamma_1 < 1$, the empirical data shown in Figs 1 and 2 has $\gamma_1 < 1$ for Ancona, and $\gamma_1 \gtrsim 1$ for Pescara. As stated above, when $\gamma_1 > 1$ the behaviour is qualitatively different: instead of having the majority of the boats nearly always fish in their home area, with occasional "jumps" to go to the neighbouring zone, there is always a degree of "mixing", as at any given time there is always a fraction $\approx 1 - \mathbb{E}\left[n_{\mathrm{A},0}\right]$ of fishermen from Ancona fishing near Pescara. For the sake of completeness Fig. 6 displays a simulation of this case, with γ_1 well above 1. This last regime is qualitatively very different to that with $\gamma_1 < 1$ and corresponding to Figs. 1 (top panel) and 3, as stressed above: there are always close to 95% of the fishermen from Ancona fishing near ththeir home port with no large collective excursions to Pescara's area.

VI. CONCLUSION

In this paper, we empirically analysed the distribution of the locations of fishing vessels in the two areas near to Ancona and Pescara. By detecting to which port a vessel belongs, we computed the fraction of fishermen fishing in their home zone and looked at their statistical properties. We found that the empirical distribution functions are well approximated by asymmetric Beta distributions, and their auto-correlations by exponentials. Inspired by such evidence, we extended Kirman and Föllmer's ants recruitment model to finite and asymmetric resources. We performed a numerical and theoretical analysis in the mean field approximation, and showed that the auto-correlations and the stationary distribution of the fraction of fishermen appear to be respectively exponential and Beta distributed. Finally, we provided the phase diagram that separates a low and high herding phase, as well as a fish extinction phase.

We have further tested our dynamics by looking at higher order correlations that can be empirically computed. This signal appears to be very noisy and of low intensity but consistent with an exponential decay, with a

timescale compatible with that predicted by our model. Given the results that we have described, we are quite confident in our minimal model since it is able to reproduce surprisingly well the generic stylized facts within a limited though behaviourally sound framework. In particular, we have shown in Appendix B that while a multi-zone model (with more than two zones) would possibility be more realistic, the results for our two-zone model can be seen as the result of the aggregation of several zones, providing solid micro-foundations to our approach and justifying our looking at two aggregated zones for empirical analysis.

ACKNOWLEDGMENTS

We thank Jean-Philippe Bouchaud, Alexandre Darmon, Mauro Gallegati and Gianfranco Giulioni for fruitful discussions and help in interpreting the data. This research was conducted within the *Econophysics & Complex Systems Research Chair*, under the aegis of the Fondation du Risque, the Fondation de l'Ecole polytechnique, the Ecole polytechnique and Capital Fund Management, and within the *New Approaches to Economic Challenges* (NAEC) OECD programme on complex systems.

[1] Garrett Hardin. The tragedy of the commons. *Science*, 162(3859):1243–1248, 1968.

[2] Stratis Gavaris. Use of a multiplicative model to estimate catch rate and effort from commercial data. *Canadian Journal of Fisheries and Aquatic Sciences*, 37(12):2272–2275, 1980.

[3] Marianne Vignaux. Analysis of vessel movements and strategies using commercial catch and effort data from the new zealand hoki fishery. *Canadian Journal of Fisheries and Aquatic Sciences*, 53(9):2126–2136, 1996.

[4] Peter M Allen and Jacqueline M McGlade. Dynamics of discovery and exploitation: the case of the scotian shelf groundfish fisheries. *Canadian Journal of Fisheries and Aquatic Sciences*, 43(6):1187–1200, 1986.

[5] Sorin Dascalu, Tudor Scurtu, Andreea Urzica, Mihai Trascau, and Adina Magda Florea. Using norm emergence in addressing the tragedy of the commons. In *International conference on computational collective intelligence*, pages 165–174. Springer, 2013.

[6] Global Fishing Watch, Fishing Vessels Dataset, `https://globalfishingwatch.org/datasets-and-code/vessel-identity`, 2020.

[7] Mauro Gallegati, Gianfranco Giulioni, Alan Kirman, and Antonio Palestrini. What's that got to do with the price of fish? buyers behavior on the ancona fish market. *Journal of Economic Behavior & Organization*, 80(1):20–33, 2011.

[8] Alan Kirman. Ants, rationality, and recruitment. *The Quarterly Journal of Economics*, 108(1):137–156, 1993.

[9] José Moran, Antoine Fosset, Michael Benzaquen, and Jean-Philippe Bouchaud. Schrödinger's ants: a continuous description of Kirman's recruitment model. *Journal of Physics: Complexity*, 1(3):035002, aug 2020.

[10] P. A. P. Moran. Random processes in genetics. *Mathematical Proceedings of the Cambridge Philosophical Society*, 54(1):60–71, 1958.

[11] Sewall Wright. Statistical genetics and evolution. *Bull. Amer. Math. Soc.*, 48(4):223–246, 04 1942.

[12] J. L. Deneubourg, S. Aron, S. Goss, and J. M. Pasteels. The self-organizing exploratory pattern of the argentine ant. *Journal of Insect Behavior*, 3(2):159–168, March 1990.

[13] R. Beckers, J. L. Deneubourg, S. Goss, and J. M. Pasteels. Collective decision making through food recruitment. *Insectes Sociaux*, 37(3):258–267, September 1990.

[14] Gary S. Becker. A note on restaurant pricing and other examples of social influences on price. *Journal of Political Economy*, 99(5):1109–1116, 1991.

[15] David S. Scharfstein and Jeremy C. Stein. Herd behavior and investment. *The American Economic Review*, 80(3):465–479, 1990.

[16] Robert J. Shiller and John Pound. Survey evidence on diffusion of interest and information among investors. *Journal of Economic Behavior & Organization*, 12(1):47–66, August 1989.

[17] Thomas Lux. Herd behaviour, bubbles and crashes. *The Economic Journal*, 105(431):881, July 1995.

[18] Robert MacArthur. Species packing and competitive equilibrium for many species. *Theoretical population biology*, 1(1):1–11, 1970.

[19] Robert Mac Arthur. Species packing, and what competition minimizes. *Proceedings of the National Academy of Sciences*, 64(4):1369–1371, 1969.

[20] Nicolas Bacaër. *Lotka, Volterra and the predator–prey system (1920–1926)*, pages 71–76. Springer, 2011.

[21] Hannes Risken. Fokker-planck equation. In *The Fokker-Planck Equation*, pages 63–95. Springer Berlin Heidelberg, 1996.

[22] Milton Abramowitz and Irene A Stegun. *Handbook of mathematical functions with formulas, graphs, and mathematical tables*, volume 55. US Government printing office, 1948.

Appendix A: Full dynamical solution

The goal of this section is to sketch a full dynamical solution for the dynamics of Eq. (16). We drop the indices A or P for clarity, obtaining:

$$\frac{\mathrm{d}n}{\mathrm{d}t} = \mu(\gamma_0 - (\gamma_0+\gamma_1)n) + \sqrt{2\mu n(1-n)}\eta(t), \tag{A1}$$

a stochastic differential equation that corresponds to the following Fokker-Planck equation [21]:

$$\partial_t \rho = \mu\partial_{nn}(n(1-n)\rho) - \mu\partial_n((\gamma_0 - (\gamma_0+\gamma_1)n)\rho), \tag{A2}$$

with reflecting boundary conditions in $n=0$ and $n=1$.

As in Ref. [9], one can "diagonalize" this equation, writing it as:

$$\partial_t \rho = \mathscr{A}\rho, \tag{A3}$$

with $\mathscr{A}$ a Fokker-Planck operator that gives the right-hand side of Eq. (A2) when applied to ρ. It is in principle possible to apply the same techniques as in Ref. [9] to obtain a Schrödinger's equation for an alternative function Ψ, that one could then use to compute ρ explicitly.

However, one can also solve the eigenvalue problem $\mathscr{A}\rho_{\mathscr{E}} = \mathscr{E}\rho_{\mathscr{E}}$, so that the general solution for ρ reads:

$$\rho(n,t) = \sum_{\mathscr{E}} \lambda_{\mathscr{E}}\rho_{\mathscr{E}}(n)e^{-\mathscr{E}t}. \tag{A4}$$

In this setting, $\mathscr{E}$ and $\rho_{\mathscr{E}}$ are respectively the eigenvalues and eigenvectors of the operator $\mathscr{A}$. These eigenvectors should also be normalized so that the integral of ρ is equal to 1.

The problem therefore translates into finding functions $\rho_{\mathscr{E}}$ and numbers (or "energies") $\mathscr{E}$ that satisfy:

$$\mu\mathscr{E}\rho_{\mathscr{E}} = \mu\partial_{nn}(n(1-n)\rho_{\mathscr{E}}) - \mu\partial_n((\gamma_0 - (\gamma_0+\gamma_1)n)\rho_{\mathscr{E}}) \tag{A5a}$$

$$J_{\mathscr{E}}(0) = J_{\mathscr{E}}(1) = 0 \tag{A5b}$$

$$\int_0^1 \mathrm{d}n\ \rho_{\mathscr{E}}(n) < \infty, \tag{A5c}$$

with $J_{\mathscr{E}}(n) = \mu\partial_n(n(1-n)\rho_{\mathscr{E}}) - \mu(\gamma_0 - (\gamma_0+\gamma_1)n)\rho_{\mathscr{E}}$.

In order to solve Eq. (A5a), we rewrite it as:

$$n(1-n)\rho''_{\mathscr{E}} + (2-\gamma_0 - (4-\gamma_0-\gamma_1)n)\rho'_{\mathscr{E}} - (2+\mathscr{E}-\gamma_0-\gamma_1)\rho_{\mathscr{E}} = 0 \tag{A6}$$

The solutions of this differential equation are given in terms of the hypergeometric function:

$${}_2F_1(a,b;c;n) = \sum_k \frac{(a)_k(b)_k}{(c)_k}\frac{n^k}{k!}, \quad (a)_k = \prod_{i=0}^{k-1}(a+i). \tag{A7}$$

Here the two linear independent solutions well defined around zero, see [22], are ${}_2F_1(a,b;2-\gamma_0;n)$ and $n_2^{\gamma_0-1}F_1(a+\gamma_0-1, b+\gamma_0-1;\gamma_0;n)$, where a,b are the solutions of:

$$a+b = 3-\gamma_0-\gamma_1 \tag{A8a}$$

$$ab = 2+\mathscr{E}-\gamma_0-\gamma_1. \tag{A8b}$$

Only the second solution cited above verifies the boundary condition at $n=0$. Applying then an Euler transformation[8] on this solution leads to:

$$\rho_{\mathscr{E}}(n) = C_{\mathscr{E}} n^{\gamma_0-1}(1-n)^{\gamma_1-1}\,{}_2F_1(1-a,1-b;\gamma_0;n), \tag{A9}$$

[8] The Euler transformation for the hypergeometric function states that ${}_2F_1(a,b;c;n) = (1-n)_2^{c-a-b}F_1(c-a,c-b;c;n)$.

with $C_{\mathscr{E}}$ a constant. This solution is well defined at $n = 1$ and also verifies the boundary condition. To check the integrability condition one can compute explicitly

$$\int_0^1 \mathrm{d}n\ \rho_{\mathscr{E}}(n) = C_{\mathscr{E}} \sum_k \frac{(1-a)_k(1-b)_k \Gamma(\gamma_0+k)\Gamma(\gamma_1)}{(\gamma_0)_k \Gamma(\gamma_0+\gamma_1+k)k!}, \tag{A10}$$

with Γ the Gamma function. If $1-a$ is a non-negative integer[9] all terms in the series are non-zero. Using then $(x)_k \propto \Gamma(x+k)$ together with the Stirling formula $\Gamma(x+1) \approx \sqrt{2\pi}x^{x+1/2}e^{-x}$ for $x \gg 1$, we find that the general term of the series converges to a constant when $k \to +\infty$ and therefore that $\int_0^1 \mathrm{d}n\ \rho_{\mathscr{E}}(n) = +\infty$. Therefore, the condition that the functions $\rho_{\mathscr{E}}$ have a finite integral implies that there exists a positive integer k such that $1-a = -k$, and so also that $b = 2-k-\gamma_0-\gamma_1$ and $\mathscr{E} = -k(\gamma_0+\gamma_1+k-1)$. Since the numbers $\mathscr{E}$ are discrete, and are indexed by k, we write $\rho_k := \rho_{\mathscr{E}_k}$.

In conclusion, the eigenvectors ρ_k and eigenvalues $\mathscr{E}_k$ are discrete and given by:

$$\mathscr{E}_k = -k(\gamma_0+\gamma_1+k-1) \tag{A11}$$

$$\rho_k(n) = C_k n^{\gamma_0-1}(1-n)^{\gamma_1-1}\,{}_2F_1(-k, \gamma_0+\gamma_1+k-1; \gamma_0; n), \tag{A12}$$

which allows then for a solution of the form given in Eq. (A4).

There only remains to find the coefficients $\lambda_{\mathscr{E}}$ that depend on the initial condition. This can be done by transforming the Fokker-Planck equation into a Schrödinger's equation as in Ref. [9], noticing that the solutions to said Schrödinger equation can be found in terms of the eigenvalues and eigenvectors ρ_k, and one can therefore find the coefficients $\lambda_{\mathscr{E}}$ by projecting the initial condition onto the orthogonal set of eigenvectors of the Schrödinger operators, see the Appendices in Ref. [9] for a detailed technical explanation.

Appendix B: A symmetric multizones extension

Here we present a very natural extension of our model to the general case of M symmetric zones with finite resources. Without loss of generality we set $C_\varepsilon = 1$ to have lighter notations, but this doesn't change our main message. We also introduce the vector notations $\mathbf{n}(t) = (n_1(t), \ldots, n_M(t))$ and $\mathbf{m}(t) = (m_1(t)\ldots, m_M(t))$, where the index accounts for the zone, and call $p_{j\to i}(\mathbf{n}(t), \mathbf{m}(t))$ the infinitesimal probability that an agent initially present in zone j at time t moves to zone i at $t+dt$. It follows that the evolution of $\mathbf{n}$ and $\mathbf{m}$ is given by:

$$\mathrm{d}m_i(t) = m_i(t)(\nu(1-m_i(t)) - \beta n_i(t))\mathrm{d}t \tag{B1}$$

$$p_{j\to i}(\mathbf{n}(t), \mathbf{m}(t)) = \frac{n_j(t)N}{M-1}\left[\varepsilon f\left(m_j(t)\right)\right] + \mu N^2 n_i(t) n_j(t). \tag{B2}$$

Introducing for simplicity $h(n,m) = m(\nu(1-m) - \beta n)$, the joint density ρ of the variables $(\mathbf{n}(t), \mathbf{m}(t))$ evolves according to the following Fokker-Planck equation:

$$\begin{aligned}\partial_t \rho(\mathbf{n}, \mathbf{m}) = &-\sum_i \partial_{m_i}(h(n_i, m_i)\rho) + \sum_{i\neq j}\left(\partial_{n_i} - \partial_{n_j}\right)\left(\frac{\varepsilon f\left(m_j\right)}{M-1} n_j \rho\right) \\ &+ \mu \sum_{i\neq j}\left(\partial_{n_i n_i} - \partial_{n_j n_i}\right)\left(n_i n_j \rho\right).\end{aligned} \tag{B3}$$

[9] As the hypergeometric function is symmetric with respect to its two first arguments, we restrict our analysis to the first one only.

Owing to the symmetry of the problem, one may generalize the argument used in Section IV to obtain the stationary averages:

$$\mathbb{E}[n_i] = \frac{1}{M}, \quad \mathbb{E}[m_i] = \left(1 - \frac{\beta}{M\nu}\right)_+ \tag{B4}$$

with $(x)_+$ the positive part of x. This again shows the existence of an extinction regime whenever $\beta = M\nu$. In what follows we assume that $\beta/\nu < 1/M$, to study the behaviour of the system outside of extinction.

When $\kappa = 0$ the density of $\boldsymbol{n}$ is a Dirichlet distribution with all parameters equal to (ε/δ), namely:

$$\rho_{\boldsymbol{n}}(n_1, \ldots, n_M) = \left(\prod_{i=1}^{M} n_i^{\varepsilon/\mu}\right) \mathbf{1}_{\{\sum_{i=1}^{M} n_i = 1\}}. \tag{B5}$$

As argued previously, whenever the noise-level is coupled to the fish population with $\kappa > 0$, we postulate that the solution can be approximated by a Dirichlet distribution with all parameters set to $(\tilde{\varepsilon}/\mu)$ with $\tilde{\varepsilon} = f(1 - \frac{\beta}{M\nu})\varepsilon$.

The Dirichlet distribution has one key property: $\sum_{i \geq k} n_i$ follows a Beta distribution with parameters $(k\tilde{\varepsilon}/\mu, (M-k)\tilde{\varepsilon}/\mu)$, corresponding to the stationary state of our two-zone model. We have also checked that the mean-field approximation of Eq. B1 follows the same type of property: the variable $\sum_{i \geq k} n_i(t)$ is ruled by the mean-field approximation of Eq. (6). This result gives solid micro-foundations to our approach, and justifies our looking at two aggregated zones for empirical analysis. This likely contributes to the very good agreement found between empirical results and our model.